ICSV13 - Vienna
The Thirteenth International Congress on Sound and Vibration
Vienna, Austria, July 2-6, 2006

VIBRATION ANALYSIS OF THE TOP PLATES OF TRADITIONAL GREEK STRING MUSICAL INSTRUMENTS

M. Bakarezos[1], S. Gymnopoulos[1], S. Brezas[1], Y. Orfanos[1,2], E. Maravelakis[3], C.I. Papadopoulos[4], M. Tatarakis[5], A. Antoniadis[3] and N.A. Papadogiannis*[1]

[1]Department of Music Technology & Acoustics, T.E.I. of Crete, 1 E. Daskalaki Str., Perivolia, 74100 Rethymnon, Crete, Greece
[2]Institute of Electronic Structure & Laser, FO.R.T.H., Vassilika Vouton, P.O. Box 1527, 71110 Heraklion, Crete, Greece
[3]Department of Natural Resources & Environment, T.E.I. of Crete, 3 Romanou Str., Chalepa, 73133 Chania, Crete, Greece
[4]School of Naval Architecture & Marine Engineering, N.T.U.A., 9 Iroon Polytechniou Str., 15780 Zografou, Athens, Greece
[5]Department of Electronics Engineering, T.E.I. of Crete, 3 Romanou Str., Chalepa, 73133 Chania, Crete, Greece
npapadogiannis@stef.teicrete.gr

Abstract

This work aims at the establishment of a complete method for the prediction and evaluation of the acoustical characteristics of string instruments based on the vibrational behavior of the instruments individual parts. It is well known that the vibrational characteristics of the top plates of string instruments affect significantly their sound emission characteristics. In this respect, a method for the vibration analysis and characterization of the top plates of string instruments is reported. The method combines two experimental techniques, namely time-average Electronic Speckle Pattern Interferometry (ESPI) and impulse response analysis, as well as a theoretical finite element (FE) analysis of models of the top plates constructed by 3-dimensional laser scans. The method is applied to characterize the vibrational behavior of the top plates of various traditional Greek string instruments (Cretan lyre) but can be extended to any string instruments, such as guitars and violins. The resonance curves of the top plates extracted through impulse response measurements reveal the eigenfrequencies for each top plate, which are in excellent agreement with the observed ones with time-average ESPI. The vibration amplitude distributions (eigenmodes) obtained by time-average ESPI for each eigenfrequency are in good agreement with the predicted ones from the FE analysis.

INTRODUCTION

Acoustical characteristics of string instruments have been extensively studied over the past decades. The methods of study include several techniques, for example modal analysis using holographic interferometry [1-4], frequency response analysis [2-5] and sound spectra analysis [6]. Several types of holographic interferometry techniques have been employed for the study of the vibrational modes of musical instruments or of their individual parts. Such techniques are classical holography [7], TV holography, digital or electronic speckle pattern photography, and digital or electronic speckle pattern interferometry (DSPI or ESPI) [8-10]. Over the years the ESPI technique has been proven the most simple and straightforward technique for normal mode extraction. The holographic method that we use in this study is the time-average ESPI, with which contours of equal out-of-plane vibration amplitude can be extracted.

The results of these experimental techniques can be theoretically tested by the well-established method of finite element analysis (FEA). For the development of a FEA model capable of accurately predicting the eigenmodes and respective frequencies of a particular instrument or a part of it (e.g. a top plate), it is important to know its exact geometry and boundary conditions, as well as the elastic properties of its material.

It is well known that the vibrational characteristics of the top plates of string instruments affect significantly their sound emission characteristics [4, 5]. The aim of the present work is to apply some of the aforementioned experimental techniques in combination with a realistic FEA model, in order to study the vibrational behaviour of the top plates of a widely used traditional Greek string instrument (Cretan lyra). This is, to the best of our knowledge, the first time that such an instrument is studied by these techniques.

THE CRETAN LYRA

The Cretan lyra is a small, pear-shaped fiddle widespread in Crete and the Dodecanese. It has three strings tuned G-D-A, held upright and played by stopping the strings from the side with fingernails. The lyra is the transformation of the old lyraki (a small model of lyra), which transformation took place long ago under the influence of the violin [11]. The most common types found today are the old-style pear-shaped lyra (figure 1b) and the modern-style lyra (figure 1a). A section through a typical lyra at the bridge is shown in figure 1c. It is worth noting that, contrary to the violin, the soundpost connects the edge of the bridge directly to the back plate. Furthermore, instead of the f-holes found in a violin, the lyra has a pair of holes, each having the shape of a part of an ellipse.

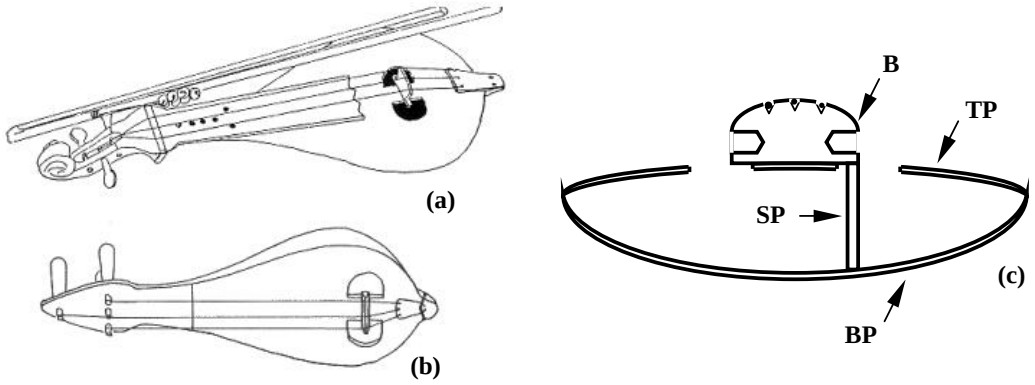

Figure 1 – (a) modern-style lyra, (b) old-style pear-shaped lyra and (c) cross section at the bridge: TP marks top plate; BP, back plate; B, bridge; and SP, soundpost.

EXPERIMENTAL TECHNIQUES & RESULTS

For the experiments with the impulse response technique a commercially available system was used (Symphonie Measuring System by 01dB-Stell), which comprises of an excitation transducer (impact hammer force transducer) and a detection transducer (accelerometer) connected to an acquisition unit. These devices are controlled by a PC with special acquisition and frequency analysis software. The object under test is impulsively excited by the impact hammer, which through feedback allows for the excitation force to be measured. The accelerometer is mounted on the object and is used to measure its response. Both the excitation and response signals are input to the software through the acquisition unit and are used to measure the, calibrated to the excitation, frequency response of the test object.

With the impulse response technique the cross transfer frequency function, $H2$, is measured:

$$H2 = \frac{\left| \int_{-\infty}^{+\infty} y(t) e^{-i2\pi f t} dt \right|^2}{\left(\int_{-\infty}^{+\infty} x(t) e^{-i2\pi f t} dt \right) \left(\int_{-\infty}^{+\infty} y(t) e^{-i2\pi f t} dt \right)^*}, \qquad (1)$$

where $y(t)$ is the accelerometer detection signal and $x(t)$ is the impact hammer excitation signal. The resulting graphical representation of the frequency response corresponds to the modulus of $H2$ (in dB through $20\log(|H2|)$ vs. frequency.

The measurement procedure is repeated several times for various positions of the accelerometer on the top plate, and the average response is calculated.

The intrerferometric method used is the time-average ESPI. The experimental set-up is schematically shown in figure 2. The beam from a cw, 100mW, single longitudinal mode laser (wavelength λ = 532nm) is split in two by means of an 80-20 beamsplitter. The former part of the beam is used to illuminate the object (object beam), after appropriate spatial expansion. The latter part of the beam is used as the reference. The reference beam is uniformly expanded by a ×20 beam expander, in order to uniformly illuminate the CCD camera detector (1392×1040 pixels). The reflected object beam is collected by a 25mm F1.4 lens attached to the camera. Care was taken for the image of the object on the CCD to have the same size as that of the reference beam. The energy of the reference beam can be varied by means of a variable neutral density filter wheel. The output of the CCD camera was directly input in the IEEE port of a PC. Special software was developed for both the on-line capturing and analysis of the images and the control of the camera functions. The object is excited by means of a piezoelectric transducer, which is controlled by a variable low-distortion frequency signal generator and a low-distortion power amplifier (Brüel & Kjaer Type 2718).

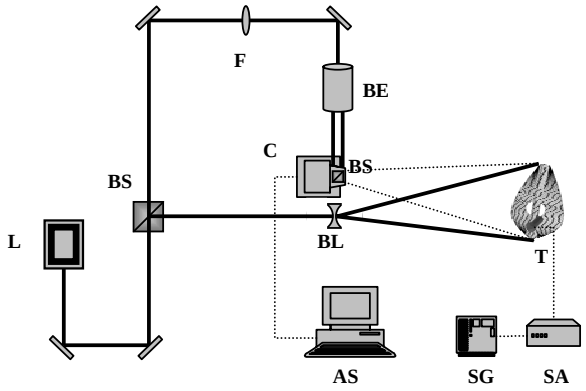

Figure 2 – ESPI experimental set-up: L marks laser source; BS, 80-20 beamsplitter; F, variable neutral density filter; BE, ×20 beam expander; C, IEEE CCD camera; BL, bi-concave lens; T, PZ transducer; AS, on-line data acquisition & analysis system; SG, variable frequency signal generator and SA, signal amplifier.

Assuming that the out-of-plane vibration across the object surface is of the form:

$$w(x,y,t) = A(x,y)\cos\left[\omega t + \phi_0(x,y)\right], \tag{2}$$

the total intensity distribution of the light incident on the detector during the camera exposure time, τ, is given by:

$$I_1 = \frac{1}{\tau}\int_0^{\tau}\left\{ I_A + I_B + 2\sqrt{I_A I_B}\cdot\cos\left[\phi + \frac{2\pi}{\lambda}\left(1+\cos\theta\right)A\cos(\omega t + \phi_0)\right]\right\}dt\,, \tag{3}$$

where I_A and I_B are the intensity distributions of the object and reference beam respectively, ϕ is the phase difference between the object and reference beam, ϕ_0 is the phase distribution of the vibration, θ is the angle between the illumination and the observation directions of the object (in our experiments $\theta \approx 0^\circ$), A is the vibration amplitude distribution of the object and ω the angular frequency of the vibration. Setting $\Gamma = (2\pi/\lambda)(1+\cos\theta)$ and $\tau = 2m\pi/\omega$, where m is an integer, equation (3) becomes [9, 10, 12]:

$$I_1 = I_A + I_B + 2\sqrt{I_A I_B}\left|(\cos\phi)J_0(\Gamma A)\right|. \tag{4}$$

where J_0 is a zeroth order Bessel function of the first kind. Note that because of time-averaging the phase of the vibration is cancelled out. As the vibration of the object continues, we assume that the vibration amplitude changes by a small amount, because of any kind of instability, from A to $A+\Delta A$. A second image is now recorded, the light intensity of which can be similarly expressed, after a Taylor expansion, as [12]:

$$I_2 = I_A + I_B + 2\sqrt{I_A I_B}\left|(\cos\phi)\left[1-\frac{1}{4}\Gamma^2(\Delta A^2)\right]J_0(\Gamma A)\right|. \tag{5}$$

The images, I_1 and I_2, are two subsequent images recorded by our system. Subtracting any two such images (i.e. subtracting I_1 from I_2) using our software, the resulting image intensity can be expressed as:

$$I = I_2 - I_1 = \frac{\sqrt{I_A I_B}}{2}\left|(\cos\phi)\Gamma^2(\Delta A^2)J_0(\Gamma A)\right|. \tag{6}$$

From equation (6) it is obvious that the time-averaged interference pattern I consists of a speckle pattern in which the contrast is modulated by the Bessel function $\left|J_0(\Gamma A)\right|$. The alternating bright and dark fringes correspond to contour lines of equal vibration amplitude. Maxima of $\left|J_0(\Gamma A)\right|$ correspond to bright fringes, with the brightest fringe being a node (A=0), while successive bright fringes of progressively decreasing brightness correspond to amplitude values 0.3λ, 0.56λ, 0.81λ, 1.07λ…

The image intensity, $I(x,y)$, described in equation (6) is on-line monitored as the excitation frequency is varied. Several images are recorded at specific frequency intervals (typically a few Hz). In this way the frequency where a normal mode appears can be accurately measured. As the excitation frequency is tuned closer to a modal frequency, the number of visible fringes increases (denoting increase of the vibration amplitude) while the fringe visibility improves.

Three different top plates have been extensively studied using the above experimental techniques, namely two modern-style top plates (by makers Stagakis and Moundrianakis) and an old-style pear-shaped top plate (by maker Petrakis). All three top plates were made of Lebanese cedar, with the wood fibre direction oriented

along the same principal axis (parallel to the larger dimension of the top plates). Typical experimental results for a modern-style top plate (Stagakis) are shown in figure 3.

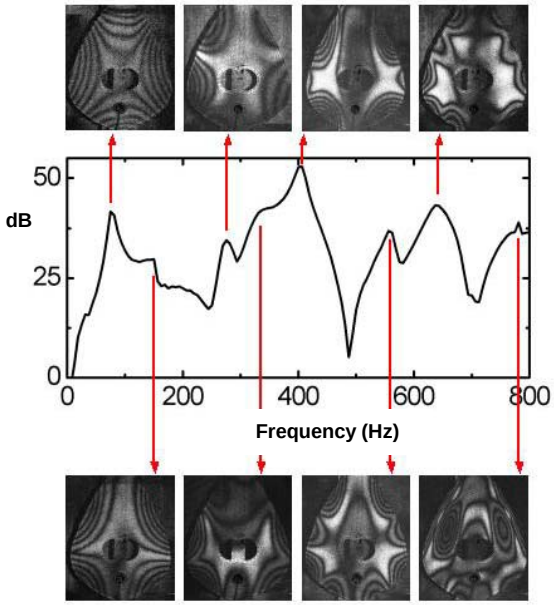

Figure 3 – Experimental techniques results: the graph shows the measured frequency response; the images are the modal shapes measured by ESPI.

The peaks in the frequency response graph correspond to the eigenfrequencies of the top plate. The images show the modal shapes, as they were determined by the ESPI technique. Although the two experimental techniques were applied independently, the eigenfrequencies extracted by the two techniques are in excellent agreement.

FEA MODEL & RESULTS

The FEA model of the top plates of various Cretan lyra styles is based on 3D scans of the top plates and is constructed with 3D hexahedral and widget solid elements. Depending on the size of the top plate, the model consists of a certain number of nodes and elements.

The material of the top plates is assumed to be of orthotropic nature having different elastic properties towards the three principal axes. Detailed modeling of the material behavior requires the definition of nine independent engineering parameters, namely the moduli of elasticity E_L, E_R and E_T toward each principal axis, the Poisson ratios v_{LR}, v_{LT} and v_{RT} and the shear moduli of elasticity G_{LR}, G_{LT} and G_{RT}. For Lebanese cedar, the species of wood used for the construction of these particular top plates, orthotropic properties are found in [13]. However, the elastic properties of a

specific part are sensitive to a number of factors such as the existence of inhomogeneities (knots, grains etc.), the moisture content as well as the chemical treatment and the temperature history this specific part has undergone. In this respect, the orthotropic properties for the specific wood found in the literature were proportionally altered so that the lowest natural frequencies of the top plates under study to be matched with the experimentally evaluated ones.

In order to simulate experimental conditions, the top plates are considered to be simply supported at the top and bottom. Eigenvalue analysis in the frequency range of 0-1500Hz for the determination of the normal modes and the corresponding modal frequencies has been performed using the Lanczos solver of the commercial finite element code HKS/ABAQUS [14].

For example, vibration amplitude distributions extracted by the FEA model are shown in figure 4. In this particular case, the FEA model simulates the vibration amplitude distribution of the Stagaki modern-style top plate. The particular model consists of a total of 14285 nodes and 12076 elements. The top plate has a total volume of 109cm^3 and mass of 48.24gr. The model takes into account the additional weight of the attached piezoelectric transducer as well as its positioning.

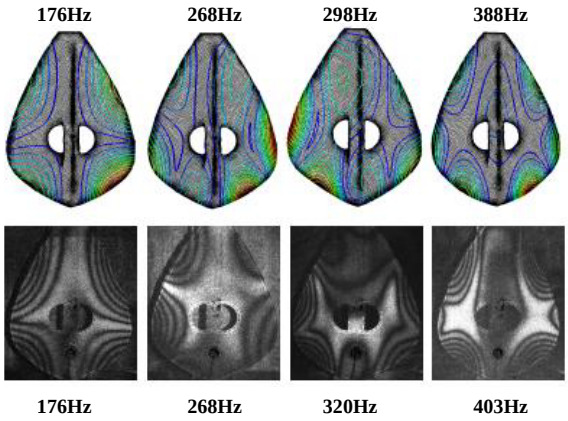

Figure 4 – Top: Typical FEA model amplitude distributions and eigenfrequencies; bottom: the corresponding ESPI modal shapes and eigenfrequencies.

DISCUSSION & CONCLUSIONS

The independent use of the impulse response technique and the ESPI technique and their excellent agreement in the eigenfrequency determination, ensures that the amplitude distribution of an eigenmode is unequivocally determined. This allows for the makers of musical instruments to preferably tune the top plates in certain frequencies, as well as to control their acoustical radiation symmetry. It is also important to notice the excellent agreement of the vibration amplitude distribution predicted by the FEA model and the one measured by ESPI (figure 4), in spite the fact that the theoretically predicted eigenfrequencies do not exactly coincide with the

experimentally measured ones. This inconsistency is attributed to the fact that the values of the elastic properties of wood may vary significantly between different applications, affected by a number of environmental and procedural factors. The developed FEA model can be an invaluable tool to the instrument makers, since they can preferentially vary the geometric characteristics and the material properties in order to estimate / improve the acoustical characteristics of the top plates before construction.

In conclusion, two different experimental techniques were applied for the measurement of the eigenmodes and respective frequencies of Cretan lyra top plates. A theoretical model was developed that confirms the experimental findings, which can be used to predict the vibration behaviour. All the above can constitute a complete method for the prediction and evaluation of the acoustical characteristics of string instruments based on the vibrational behavior of the instruments individual parts. The method can be extended to any string instruments, such as guitars and violins.

The project is co-funded by the European Social Fund and National Resources - (EPEAEK-II) ARCHIMIDIS I.

REFERENCES

[1| Lökberg O., "ESPI – The ultimate holographic tool for vibration analysis?", J. Acoust. Soc. Am., **75**, 1783-1791 (1984).

[2] Runnemalm A., Molin N-E. and Jansson E., "On operating deflection shapes of the violin including in-plane motions", J. Acoust. Soc. Am., **107**, 3452-3459 (2000).

[3] Jansson E., Molin N-E. and Saldner H.O., "On eigenmodes of the violin – Electronic holography and admittance measurements", J. Acoust. Soc. Am., **95**, 1100-1105 (1994).

[4] Fletcher N.H. and Rossing T.D., *The physics of musical instruments*. (Springer-Verlag, New York, 1999).

[5] Backus J., *The acoustical foundations of music*. (W.W. Norton & Co, New York, 1977).

[6] Cohen D. and Rossing T.D., "The acoustics of mandolins", Acoust. Sci. & Tech., **24**, 1-6 (2003).

[7] Powel R.L. and Stetson K.A., "Interferometric vibration analysis by wavefront reconstruction", J. Opt. Soc. Am., **55**, 1593-1598 (1965).

[8] Molin N-E., "Applications of whole field interferometry in mechanics and acoustics", Optics and Lasers in Engineering, **31**, 93-111 (1999).

[9] Rastogi P.K. Ed., *Digital speckle pattern interferometry and related techniques*. (John Wiley & Sons Ltd., Chichester, 2001).

[10] Jones R. and Wykes C., *Holographic and speckle interferometry*. (Cambridge University Press, Cambridge, 1989).

[11] Anogianakis F., *Greek folklore musical instruments*. (Melissa, Athens, 1991).

[12] Huang C-H. and Ma C-C., "Experimental and numerical investigations of resonant vibration characteristics for piezoceramic plates", J. Acoust. Soc. Am., **109**, 2780-2788 (2001).

[13] Forest Product Laboratory, *Wood Handbook – Wood as an engineering material, Technical report FPL-GTR-113*. (1999).

[14] Hibbit D., Karlsson & Sorensen, Inc, *Abaqus Theory Manual v. 6.5*. (2004).